

Practical Consequences of Numerical Modeling of the Near-Wellbore Stress Field for Wellbore Strengthening

Huy Huynh, Nils Kaageson-Loe & Mark W. Sanders, M-I SWACO

Copyright 2008, AADE

This paper was prepared for presentation at the 2008 AADE Fluids Conference and Exhibition held at the Wyndam Greenspoint Hotel, Houston, Texas, April 8-9, 2008. This conference was sponsored by the Houston Chapter of the American Association of Drilling Engineers. The information presented in this paper does not reflect any position, claim or endorsement made or implied by the American Association of Drilling Engineers, their officers or members. Questions concerning the content of this paper should be directed to the individuals listed as authors of this work.

Abstract

The need for wellbore strengthening technology is most acute for depleted-zone drilling and drilling extended-reach wells in deepwater environments. Numerical modeling using FLAC-2D demonstrates how the near-wellbore stress field is enhanced through the process of forming and propping fractures.

This particular modeling approach provides an additional insight into the mechanisms that may operate at the wellbore wall. The results support existing theories that have been published describing the concepts of wellbore strengthening. The modeling work confirms that the presence of an unsupported fluid-filled fracture modifies the elastic stress field surrounding the wellbore. The near-wellbore stress field is then further modified by sealing and propping the fracture. The model can be used to help determine the size of the fracture aperture necessary to enhance the wellbore strength to a predetermined level. The relative compressibility between the loss-prevention material (LPM) and the rock can be investigated with respect to fracture closure and further changes to the stress field. This information highlights critical characteristics for wellbore strengthening materials.

Introduction

Stresses around the wellbore and properties of the rock govern the pressure that can be applied inside the wellbore while drilling. The maximum pressure the wellbore can sustain is when the fluid pressure inside exceeds the near-wellbore stress at a given point on the perimeter. Above this pressure a fracture will form and propagate, compromising the integrity of the wellbore. If fracturing is anticipated, loss prevention material can be added to the drilling fluid to seal off the fracture and prevent further propagation and fluid loss.

In theory, the fracture sealing process can be modified by purposefully propping open and then sealing fractures with material. The propping action artificially enhances the near-wellbore stress field, allowing higher wellbore pressures before fracturing is initiated. This concept is known as "wellbore strengthening" and when successfully practiced can lead to significant design simplification and cost savings.

This paper presents the results of a FLAC-2D numerical modeling study on how the near-wellbore stress field is beneficially and artificially enhanced through the process of

forming and propping fractures. A relatively simple anisotropic model of a subsurface circular opening has been used to perform the investigation. A comparison between the relative wellbore strengthening effects between simulated sandstone and shale was made.

Numerical Modeling of Wellbore Strengthening Concepts

FLAC-2D was utilized in this study, primarily as this software is extensively and successfully used for two-dimensional plane-strain modeling of geologic materials, such as shale and sandstone.

A conventional concentric, isotropic circular grid was used in the simulations, with a hole in the centre of the grid representing an 8½-in. wellbore (Figure 1). The radius to the outer boundary of the grid is 10 times the simulated wellbore radius; i.e., 85-in. (216 cm). This distance minimizes any grid-edge effects on the near-wellbore stress field while maintaining relatively short computational times. The model also assumes a pre-existing 8-in. (20.3-cm) long, 100-μm wide slot-like fracture. This is simulated by removing elements in the grid and is a simplification of the fracture geometry. Further fracture propagation is assumed not to occur so the fracture tip is fixed.

Far field in-situ stresses are applied to each node of the concentric model, with the outer boundaries of the model being fixed. The minimum horizontal principal stress (sh_{min}) is applied in the north-south orientation, and the maximum principal stress (SH_{max}) in the east-west orientation. The ratio of the far field in-situ stresses (sh_{min} and SH_{max}) used in the modeling process was based upon actual field data.

The wellbore pressure (P_{wb}) from the drilling fluid is simulated by a mechanical pressure applied to the wellbore wall of the model and initially along the wall of the fracture. As a boundary condition, it is assumed for both "permeable" sandstone and "impermeable" shale, that there is a perfect filter cake formed around the wellbore wall so that no wellbore pressure is transmitted to the pore pressure within the rock due to fluid leakoff. A pore pressure is applied to the grid cells representing the formation in the model.

Modeling properties for sandstone and shale are detailed in Table 1. The tensile strength of the rock has been artificially raised to 1000 psi from a few 100 psi to prevent tensile

yielding of the rock thus preserving the elastic stress state. In so doing the contrast in the tensile stress around the wellbore is more easily observed.

The process of wellbore strengthening by propping open a fracture is simulated by “inserting” an incompressible plate into the fracture at a rate of 0.4 mm/s until the desired propping depth is achieved. The leading edge of the plate is wedge-shaped widening from the tip, over a distance of 8 mm, to 400 μm in width (Figure 2). Once the wedge is in place the model is cycled for a further 2,500 iterations in order to attain near-equilibrium for stresses and strains.

Fluid pressure within the fracture is set according to the condition being simulated. In the case of a free fracture, i.e., a fracture is present but not filled, the fluid pressure is equated with the wellbore pressure (27 MPa = 270 bar = 3,916 psi). Where the fluid in the fracture becomes isolated from the wellbore by the insertion of the fracture propping wedge, the fluid pressure within the fracture interior is either set equal to the pore pressure if sandstone properties are assumed (18 MPa = 180 bar = 2,610 psi), or is set equal to wellbore pressure if shale properties are assumed (27 MPa = 270 bar = 3,916 psi). This is intended to simulate fluid leakoff in the case of sandstone. In all cases, it is assumed that the fluid is incompressible.

The tapered wedge was inserted to two different depths namely, over a very short interval in proximity to the fracture mouth, and secondly, by propping over a greater interval deeper in to the fracture. This allows observations to be made on how fracture propping influences the near wellbore stress field.

When simulating propping near the fracture mouth, the wedge-shaped plate was inserted to a depth of 9.5 mm (0.37-in.). By doing this the opening is essentially widened to a width of 400 μm over an interval of 1.5 mm (0.06-in.) before tapering back to 100 μm . It should be noted that the selected insertion depth of the proppant was supported by numerous laboratory experiments dealing with sealing at the fracture mouth.¹

When simulating conditions where propping occurs over a greater interval, the wedge-shaped plate was inserted to a depth of 93 mm (3.67-in.) into the fracture. In this position, the opening is widened to 400 μm over an 85 mm (3.35-in.) interval before tapering off to simulate where a greater proportion of the fracture is filled with proppant.^{2,3}

The propped fracture simulations described above were compared with two baseline simulations – one with no fracture present in the wellbore, and the other with an open, unpropped fracture present. Together the four simulations present a spectrum of how the stress and strain state around the wellbore changes in the presence of a fracture that is to varying degrees propped and sealed open.

Results

Two sets of data are presented; one representing a sandstone and the second a shale. Together the scenarios illustrate how the stress and strain state around the wellbore is affected by the formation properties and the propping of a

fracture. In terms of material properties, the largest differences occur for the bulk and shear moduli for the two different rock types being modeled. Differences also exist in how fluid pressures within the fracture are treated. Specifically, for sandstone, fluid pressure within the fracture is set equal to pore pressure, whereas, for shale, fluid pressure is set equal to wellbore pressure.

Simulated Wellbore Strengthening in Sandstone

Figures 3-5 illustrate the hoop and radial stress magnitudes for the four different simulated scenarios.

Scenario A: Circular Borehole

A conventional elastic radial stress distribution is observed for the unfractured wellbore. Here, the stress field local to the wellbore is influenced by the wellbore pressure condition: $sh_{\min} < P_{wb} < SH_{\max}$ such that relatively modest tensile hoop stresses develop in the east-west direction due to slight ovalization of the wellbore (Figure 3a). Elsewhere, the hoop stresses are either slightly tensile (red-shaded area, Figure 3a) or slightly compressive (grey-shaded area, Figure 4a) but will fall away to zero with distance from the wellbore. The radial stresses local to the borehole wall are also a consequence of the wellbore pressure (P_{wb}), which causes a slight compression just behind the wellbore wall in the north-south direction, and a moderate stress increase (red-shaded area, Figure 5a). In the east-west direction, the radial stresses local to the wellbore are equal to the wellbore pressure.

Scenario B: Circular Borehole, Unsupported Fracture

The presence of an unsupported fracture modifies the stress field around the wellbore. The modification is primarily a consequence of the fluid pressure within the fracture where this is equated to the wellbore pressure (27 MPa = 3,916 psi) assuming that a perfect filter cake is present. This causes compression of the surrounding rock (Figures 3b & 4b). As a result, the tensile hoop stresses on the western edge of the hole around the fracture are reduced to almost zero (the residual stresses are partly a result of grid effects). The radial stresses still show a localized compression of the wellbore in the north-south direction (red-shaded area, Figure 5b), but the maxima have rotated slightly to the west as a result of the net compression from the fluid in the fracture.

Scenario C: Circular Borehole, 9.5-mm Propped Fracture

In sandstone Scenario C, the fracture is supported by an incompressible wedge being inserted into the fracture to a depth of 9.5 mm. The fluid pressure within the fracture, behind the wedge, is assumed to be isolated from the wellbore and has pressure equal to the pore pressure (18 MPa = 2,610 psi). The stress field around the borehole and fracture is modified by the presence of the wedge and the lower fluid pressure in the fracture. The wedge is 400- μm wide at the fracture mouth, and its insertion compresses the surrounding rock, causing a relatively high localized compressive hoop stress at the borehole wall (blue-shaded area, Figure 4c).

Through the Poisson's Ratio effect, this compression also causes a much localized increase in radial stress (yellow-red colors, Figure 5c). The fluid pressure in the fracture behind the wedge is less than sh_{min} and thus tensile hoop stresses develop as the rock attempts to dilate (expand) to close the fracture (yellow-green-blue shading, Figure 3c).

Scenario D: Circular Borehole, 93-mm Propped Fracture

In sandstone Scenario D, the wedge is inserted into the fracture to a depth of 93 mm. The fluid pressure within the fracture, behind the wedge, is assumed to be isolated from the wellbore and has pressure equal to the pore pressure (18 MPa = 2,610 psi). The longer propping interval (nearly a third of the fracture length) and the lower fluid pressure in the fracture modify the local stress field. The wedge is 400- μ m wide along most of its length (85 mm), and its insertion compresses the surrounding rock. This causes a localized moderate compressive hoop stress around the wedge and at the borehole wall (blue-shaded area, Figure 4d). A further consequence of this compression is a localized increase in the radial stress and a rotation of the maxima from their original north-south location (Figure 5a) to a more westerly orientation (beige-shaded area, Figure 5d). The fluid pressure behind the wedge is less than sh_{min} , and thus tensile hoop stresses develop as the rock attempts to dilate (expand) to close the fracture (yellow-green-blue shading, Figure 3d). The zone of tensile stresses around the fracture is smaller than that observed for Case C (above) due to the longer propping interval in this case (compare Figures 4c and 4d).

Deformation of Rock and Borehole in Sandstone

Figure 6 illustrates the volumetric strains that develop for the four different scenarios (A – D) as the rock deforms in response to the applied stress field. In Scenario A, the circular borehole with no fracture, the ovalization of the borehole due to the applied stresses, $sh_{min} < P_{wb} < SH_{max}$, is seen as near-wellbore tensile strains in the east-west quadrant, and compressive strains in the north-south quadrants (Figure 6a). The presence of a fluid-filled fracture significantly reduces the tensile strain (Figure 6b) due to the compression from the fluid pressure. This effect is further enhanced when a wedge is inserted into the fracture compressing the surrounding material; compressive strains are observed around the wedge in Figures 6c and 6d.

Note: the fracture has an aperture of only 100 μ m; the wider black void observed surrounding the fracture in Figures 6b – 6d is a graphical artifact caused by the FLAC plotting routine and does not reflect widening of the fracture.

Simulated Wellbore Strengthening in Shale

Figures 7 – 9 illustrate the hoop and radial stress magnitudes for the four different simulated scenarios. Each of these scenarios, and their resultant FLAC models, are similar for those described previously for the sandstone.

Scenario A: Circular Borehole

A conventional elastic radial stress distribution is observed for the unfractured wellbore. Here, the near-wellbore stress field is influenced by the wellbore pressure condition ($sh_{min} < P_{wb} < SH_{max}$) and relatively modest tensile hoop stresses develop in the east-west direction as a result of slight ovalization of the wellbore (Figure 7a). Elsewhere, the hoop stresses are either slightly tensile (red-shaded area, Figure 7a) or slight to moderately compressive (grey-blue shaded area, Figure 8a), but fall away to zero with distance from the wellbore. The radial stresses local to the borehole wall are also a consequence of the wellbore pressure (P_{wb}). This causes a slight compression just behind the wellbore wall in the north-south direction, and a moderately high stress increase (yellow-green shaded area, Figure 9a). In the east-west direction the radial stresses local to the wellbore are equal to the wellbore pressure.

Scenario B: Circular Borehole, Unsupported Fracture

The presence of an unsupported fracture modifies the stress field around the wellbore where this is primarily a consequence of the fluid pressure within the fracture which is equal to the wellbore pressure (27 MPa = 3,916 psi). This causes compression of the surrounding rock, and thus reduces the magnitude of tensile stresses on the western edge of the borehole wall (compare Figures 7a & 8a; 7b & 8b). The radial stresses still show a localized compression of the wellbore in the north-south direction (red-shaded area, Figure 9b) but the maxima have rotated slightly to the west as a result of the net compression from the fluid in the fracture.

Scenario C: Circular Borehole, 9.5-mm Propped Fracture

In shale Scenario C, the fracture is supported by a wedge being inserted into the fracture to a depth of 9.5 mm. The fluid pressure within the fracture, behind the wedge, is assumed to be isolated from the wellbore, but retains its original pressure of 27 MPa (3,916 psi) as the fluid is prevented from leaking off by the assumption that the shale has zero permeability and that the fracture can not propagate. The stress field around the borehole and fracture is therefore modified by the presence of the wedge and the high fluid pressure. The wedge compresses the surrounding rock, causing a localized high compressive hoop stress at the borehole wall (blue-shaded area, Figure 8c). Immediately behind the wedge is a small zone of tensile stresses – possibly induced by edge effects around the wedge tip. Through the Poisson's Ratio effect this compression also causes a much localized increase in radial stress, thus reducing the tensile radial stresses around the fracture (note contour lines, Figure 9c).

Scenario D: Circular Borehole, 93-mm Propped Fracture

In shale Scenario D, the wedge is inserted into the fracture to a depth of 93 mm. The fluid pressure within the fracture, behind the wedge, is assumed to be isolated from the wellbore but retains its original pressure of 27 MPa (3,916 psi). The longer propping interval modifies the stress field local to the

fracture as its insertion compresses the surrounding rock. In the shale this causes a moderate compressive stress around the wedge and at the borehole wall (blue-shaded area, Figure 8d). A further consequence of this compression is an increase in the radial stress localized to the fracture (note contour lines and red-shaded area, Figure 9d).

Deformation of Rock and Borehole in Shale

Figure 10 illustrates the volumetric strains that develop for the four different scenarios as the rock responds to the applied stress field. In Scenario A, the circular borehole with no fracture, the ovalization of the borehole due to the applied stresses, ($sh_{min} < P_{wb} < SH_{max}$) is seen as near-wellbore tensile strains in the east-west quadrant and compressive strains in the north-south quadrants (Figure 10a). The presence of a fluid-filled fracture significantly reduces the tensile strain (Figure 10b) due to the additional compression from the fluid pressure. This effect is further enhanced when an incompressible wedge is inserted into the fracture compressing the surrounding material; compressive strains (yellow-shaded area) are observed around the wedge in Figures 10c and 10d.

Note: the fracture has an aperture of only 100 μm ; as with the sandstone models, the wider black void observed surrounding the fracture in Figures 10b – 10d is a graphical artifact caused by the FLAC plotting routine and does not reflect widening of the fracture.

Discussion

Comparing the results between sandstone (Figures 3–5) and shale (Figures 7–9), it can be seen that the presence of a fracture and insertion of an incompressible wedge into the fracture does indeed modify the stress field around the wellbore. The comparisons are more clearly illustrated in Figure 11 which shows, for the four different cases, the changes in hoop stress with radial distance in the rock parallel to the fracture. Rock properties, notably bulk modulus and shear modulus, have secondary but important effects.

The presence of an unsupported fluid-filled fracture is seen to modify the elastic stress field surrounding the borehole principally by reducing the tensile hoop stresses local to the wellbore wall (Figures 11a and 11b). Tensile stresses are observed to develop at the end of the fracture. These are caused by a hinge effect arising from the fixed location of the fracture tip. The stress field is further modified when a wedge is inserted into the fracture (Figures 11c and 11d). This occurs because the wedge (in the models used here) is wider than the original fracture (400 vs 100 μm) and thus compresses the surrounding rock. The compression suppresses the tensile stresses in the fracture and the wellbore adjacent to the inserted wedge; the longer the wedge the greater the zone of influence. Close inspection of the simulation results show that significantly higher compressive hoop stresses are generated when propping over a shorter interval (9.5-mm) but that these are concentrated in a very much smaller volume. The stresses generated by the 9.5-mm long wedge are more than three times as great as those generated by the 93-mm wedge.

For the sandstone, once the wedge is inserted, the fluid

pressure in the interior of the fracture is reduced to the formation pressure to simulate leak-off. In the case of the short wedge (9.5 mm) this decrease in fluid pressure causes a significant tensile stress to develop as the surrounding rock attempts to close the opening (Figure 11c). A further noteworthy consequence is the very steep stress gradient that exists in the rock adjacent to the inserted wedge – here over a distance of 50 mm, the hoop stresses range from –12 MPa (compression) to 6 MPa (tension). For the shale where fluid leakoff does not occur, the original wellbore pressure is preserved in the fracture and the consequent hoop stress profile behind the wedge is very similar to that of the unsupported fracture (Figure 11b). In reality, wellbore pressures are unlikely to be preserved within the fracture even in shale as the fluid will eventually find a way to leak off either through further fracture propagation or leakoff through the fracture plug.

In contrast to the above, and as mentioned previously, the insertion of the 93-mm long wedge generates a more extensive compressive stress field in the rock neighboring the wedge. This superimposes and interferes with the pre-existing tensile stresses near the fracture tip and effectively accentuates them (compare Figure 11b and 11d). In the case of the sandstone, the lower fluid pressure in the fracture and resulting fracture closure further enhance the tensile stresses. It should be emphasized however that in reality the fracture tip is not fixed and that the tensile stresses will be dissipated through fracture closure and by some fracture propagation.

The modeling work has assumed some default values that represent shale and sandstone. The principal differences in these material properties are the cohesion, tension and friction values, but more importantly, the bulk and shear moduli. The former set of properties relates to rock failure and as no rock failure occurs in these simulations, then they have little bearing on the stress distribution around the wellbore. In contrast, the bulk and shear moduli determine how an elastic material will deform under an applied stress field. Bulk modulus determines how a material will change in volume and the shear modulus determines how the material will distort (shear). The greater the moduli values, the greater the material's stiffness and resistance to deformation. In Table 1 the moduli values for sandstone are much greater than those given for shale. This translates to much higher compressive hoop stresses being generated for the sandstone material when a wedge is inserted into the fracture due to the higher bulk modulus values (e.g. compare sandstone and shale in Figure 11). Also, the compression caused by the wedge will have a shear component (particularly at the wellbore wall) that transposes to the generation of radial compressive stresses through the shear modulus (Poisson's effect). Here the contrast in shear modulus values is not as great as for the bulk modulus, so the magnitudes of the radial stress are more similar for the sandstone and shale materials (compare Figures 5c and 5d and 9c and 9d).

It should be noted that the bulk and shear moduli values used in this study are only example values for sandstone and shale and are used for illustration only. A more detailed

parametric sensitivity study that would more closely approximate the full range of moduli values encountered for sand and shale was not included in this current investigation.

Conclusions

- A relatively simple anisotropic model of borehole stresses has been used to perform a preliminary investigation on wellbore strengthening in sandstone and shale.
- The modeling has attempted to demonstrate the process of beneficially modifying the near-wellbore stress field by propping an open fracture.
- The modeling work indicates that the presence of an unsupported fluid-filled fracture is seen to modify the elastic stress field surrounding the borehole.
- The near-wellbore stress field is further modified when a wedge is inserted into the fracture. This occurs because the wedge (in the models used here) is wider than the fracture and thus compresses the surrounding rock. The compression suppresses the tensile stresses in the rock in the immediate locality of the wedge.
- The longer the wedge the greater the zone of influence and the more the hoop stresses around the fracture and wellbore become compressive. This is beneficial with respect to wellbore strengthening. In contrast, and arguably equally beneficial, the highest compressive hoop stresses are generated when propping the fracture over a short interval near the wellbore wall but these are concentrated in a much smaller rock volume relative to

the stress changes caused when propping over longer intervals.

- The bulk and shear moduli are critical parameters that determine the magnitude of the compressive hoop and radial stresses that are generated when the wedge is inserted into the fracture.

Acknowledgments

The authors would like to thank the management of M-I SWACO, together with members of the M-I SWACO Fracture Studies JIP for permission to publish this paper. Thanks are also extended to Mike Stephens for useful comments made during this study.

References

1. Hettema, M., Horsrud, P., Taugbøl, K., Friedheim, J., Huynh, H., Sanders, M.W. and Young, S. "Development of an Innovative High-Pressure Testing Device for the Evaluation of Drilling Fluid Additives within Fracture Permeable Zones." OMC Paper 041/dlg2, Offshore Mediterranean Conference, Ravenna, Italy, March 28-30, 2007.
2. Dupriest, F.E. "Fracture Closure Stress (FCS) and Lost Returns Practices." SPE 92192, SPE/IADC Drilling Conference, Amsterdam, February 23-25, 2005.
3. Fuh, G.-F., Beardmore, D. and Morita, N. "Further Development, Field Testing, and Application of the Wellbore Strengthening Technique for Drilling Operations." SPE 105809, SPE/IADC Drilling Conference, Amsterdam, February 20-22, 2007.

Table 1 – FLAC Modeling Properties for Sandstone and Shale				
Parameter	Sandstone		Shale	
	SI	Imperial	SI	Imperial
Dry Density	2,700 Kg/m ³	169 lb/ft ³	2,700 Kg/m ³	169 lb/ft ³
Bulk Modulus	26,800 MPa	3.89 Mpsi	8,810 MPa	1.28 Mpsi
Shear Modulus	6,990 MPa	1.01 Mpsi	4,300 MPa	0.62 Mpsi
Cohesion	27.2 MPa	3,945 psi	38.4 MPa	5,570 psi
Tensile Strength	6.9 MPa	1,000 psi	6.9 MPa	1,000 psi
Friction Angle	27.8 degrees		14.4 degrees	
Stress Sign Convention	negative for compression		negative for compression	
Maximum Horizontal Stress (SH _{max})	-30 MPa	4,350 psi	-30 MPa	4,350 psi
Minimum Horizontal Stress (sh _{min})	-25 MPa	3,626 psi	-25 MPa	3,626 psi
Wellbore Pressure (P _{wb})	27 MPa	3,916 psi	27 MPa	3,916 psi

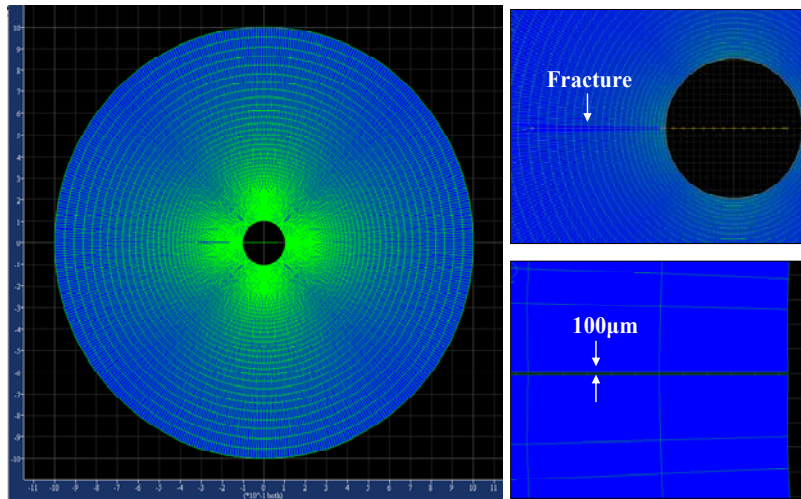


Fig. 1 – A concentric grid used to simulate stress conditions at the borehole. The fracture is a 100-μm wide slot extending 12 in. from the wellbore wall.

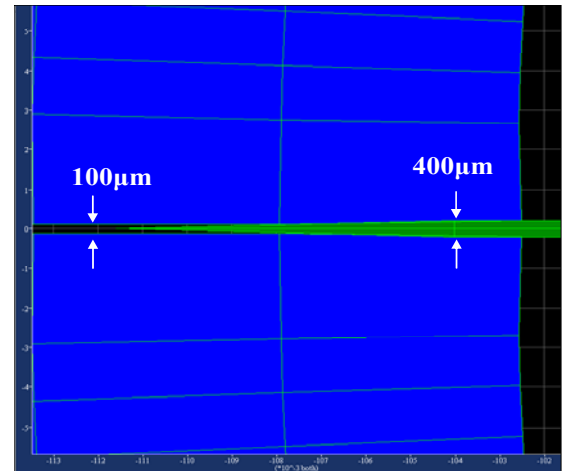


Fig. 2 – Insertion of 400-μm thick wedge into the fracture plane simulates fracture propping and wellbore strengthening.

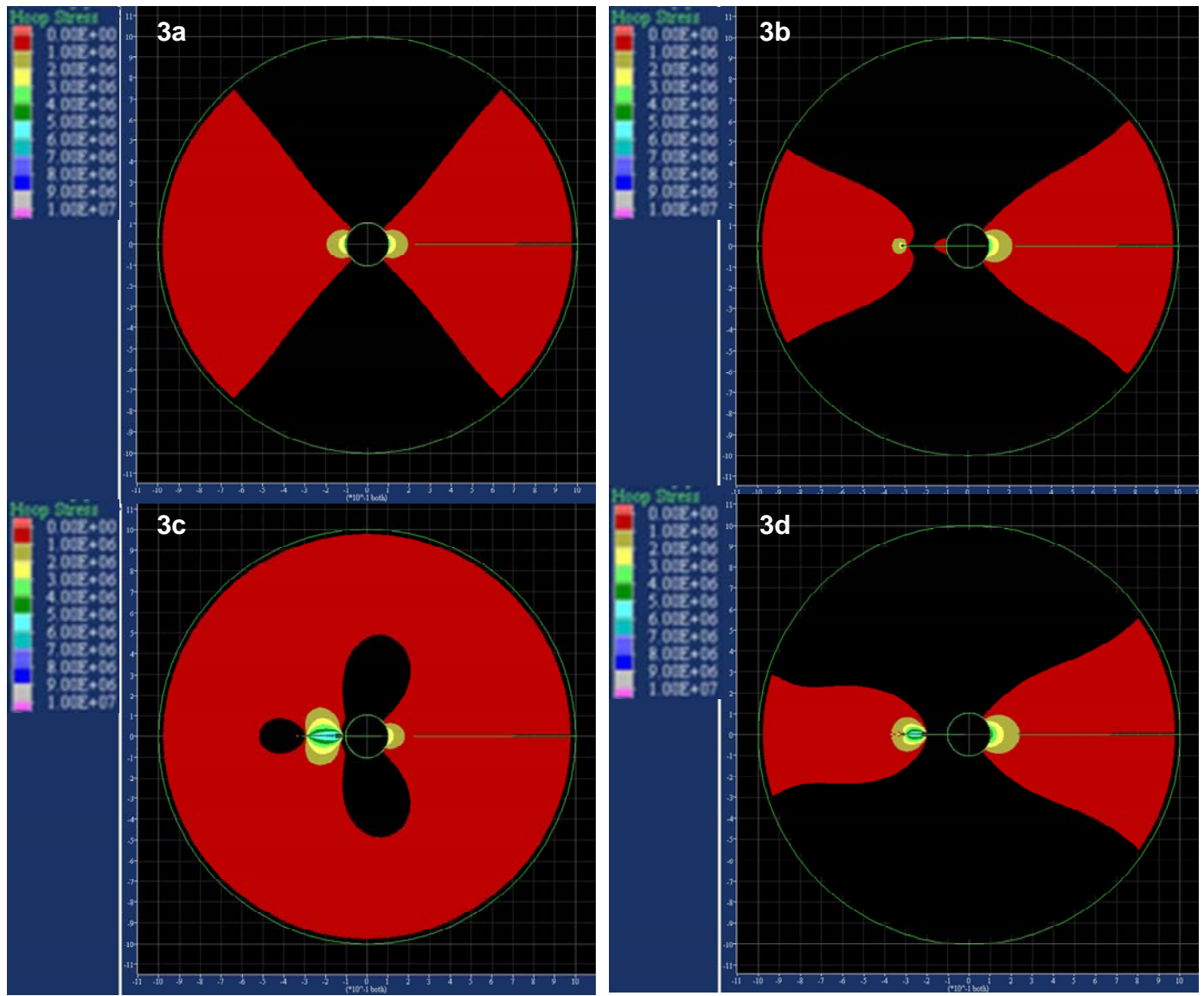


Fig. 3 – Tensile hoop stress distribution around the borehole and fracture. FLAC-2D simulations assuming sandstone properties in Table 1. Black denotes no tensile hoop stress. Red-yellow-green-blue colors denote higher stress. Stress values in key are in Pa ($1 \text{ MPa} = 10^6 \text{ Pa}$); each color change denotes a change in stress by 1 MPa. Positive values denote tensile stress. Minimum horizontal stress, sh_{\min} , oriented N-S; maximum horizontal stress, SH_{\max} , oriented E-W. **Fig. 3a** – Circular borehole; **Fig. 3b** – Circular borehole with unsupported fracture; **Fig. 3c** – Circular borehole with a propped fracture, prop length 9.5 mm; **Fig. 3d** – Circular borehole with a propped fracture, prop length 93 mm.

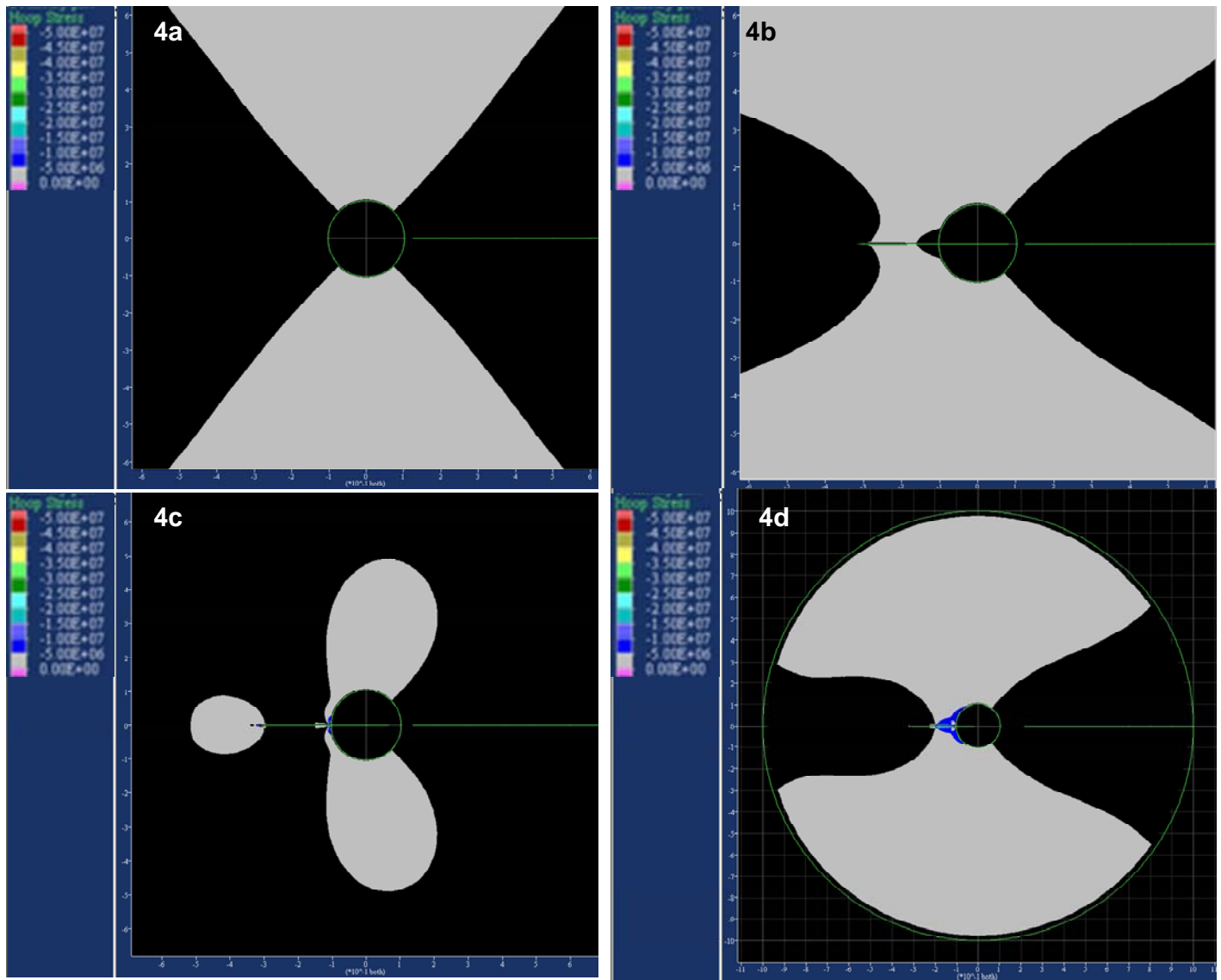


Fig. 4 – Compressive hoop stress distribution around the borehole and fracture. FLAC-2D simulations assuming sandstone properties in Table 1. Black denotes no compressive hoop stress. Yellow-blue-pink colors denote higher stress. Stress values in key are in Pa ($1 \text{ MPa} = 10^6 \text{ Pa}$); each color change denotes a change in stress by 1 MPa. Negative values denote compressive stress. Minimum horizontal stress, sh_{\min} , oriented N-S; maximum horizontal stress, SH_{\max} , oriented E-W. **Fig. 4a** – Circular borehole; **Fig. 4b** – Circular borehole with unsupported fracture; **Fig. 4c** – Circular borehole with a propped fracture, prop length 9.5 mm; **Fig. 4d** – Circular borehole with a propped fracture, prop length 93 mm.

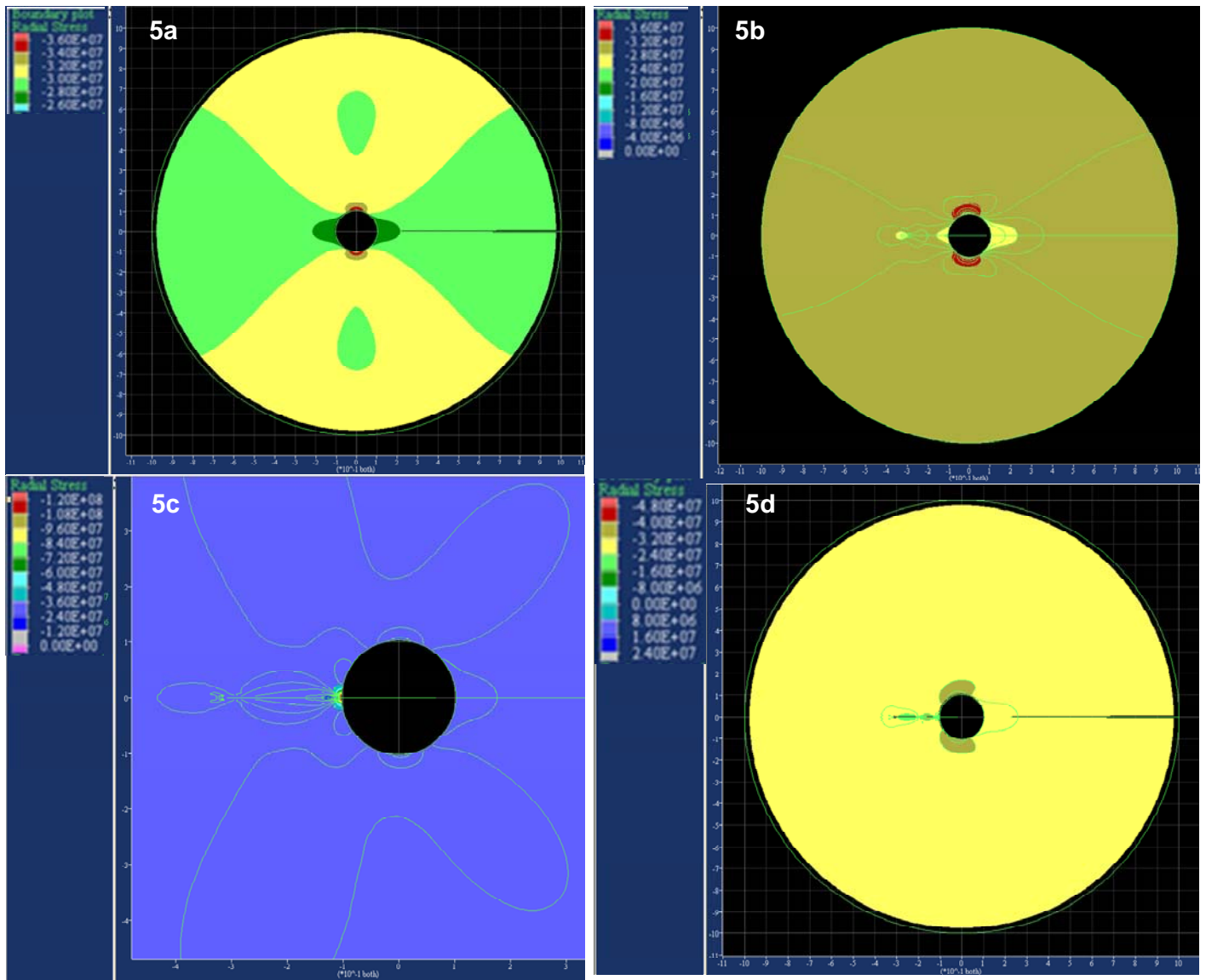


Fig. 5 – Radial stress distribution around the borehole and fracture. FLAC-2D simulations assuming sandstone properties in Table 1. Yellow-beige-red shades denote increasing radial stress; scales vary in each figure. Stress values in key are in Pa (1 MPa = 10^6 Pa). Positive values denote tensile stress and negative values denote compressive stress. Minimum horizontal stress, sh_{min} , oriented N-S; maximum horizontal stress, SH_{max} , oriented E-W. **Fig. 5a** – Circular borehole; **Fig. 5b** – Circular borehole with unsupported fracture; **Fig. 5c** – Circular borehole with a propped fracture, prop length 9.5 mm; **Fig. 5d** – Circular borehole with a propped fracture, prop length 93 mm.

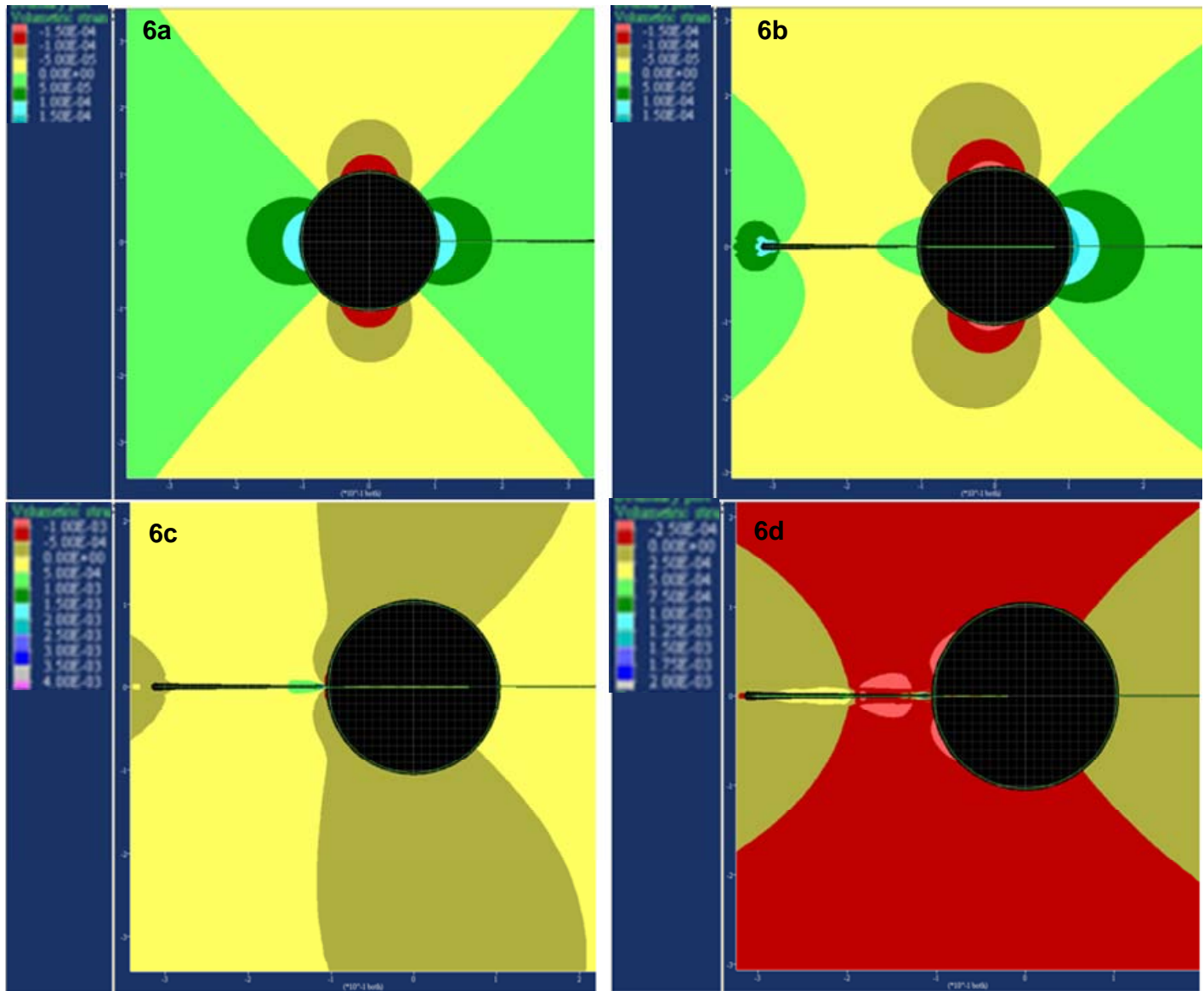


Fig. 6 – Volumetric strain around the borehole and fracture. FLAC-2D simulations assuming sandstone properties presented in Table 1. Yellow-red shades (negative values) denote volumetric compression; green-blue shades (positive values) indicate volumetric expansion (dilation). Scales vary in each figure. Strain values in key are in Percent (1 microStrain = 10^{-3} Strain%). Minimum horizontal stress, sh_{min} , oriented N-S; maximum horizontal stress, SH_{max} , oriented E-W. **Fig. 6a** – Circular borehole; **Fig. 6b** – Circular borehole with unsupported fracture; **Fig. 6c** – Circular borehole with a propped fracture, prop length 9.5 mm; **Fig. 6d** – Circular borehole with a propped fracture, prop length 93 mm.

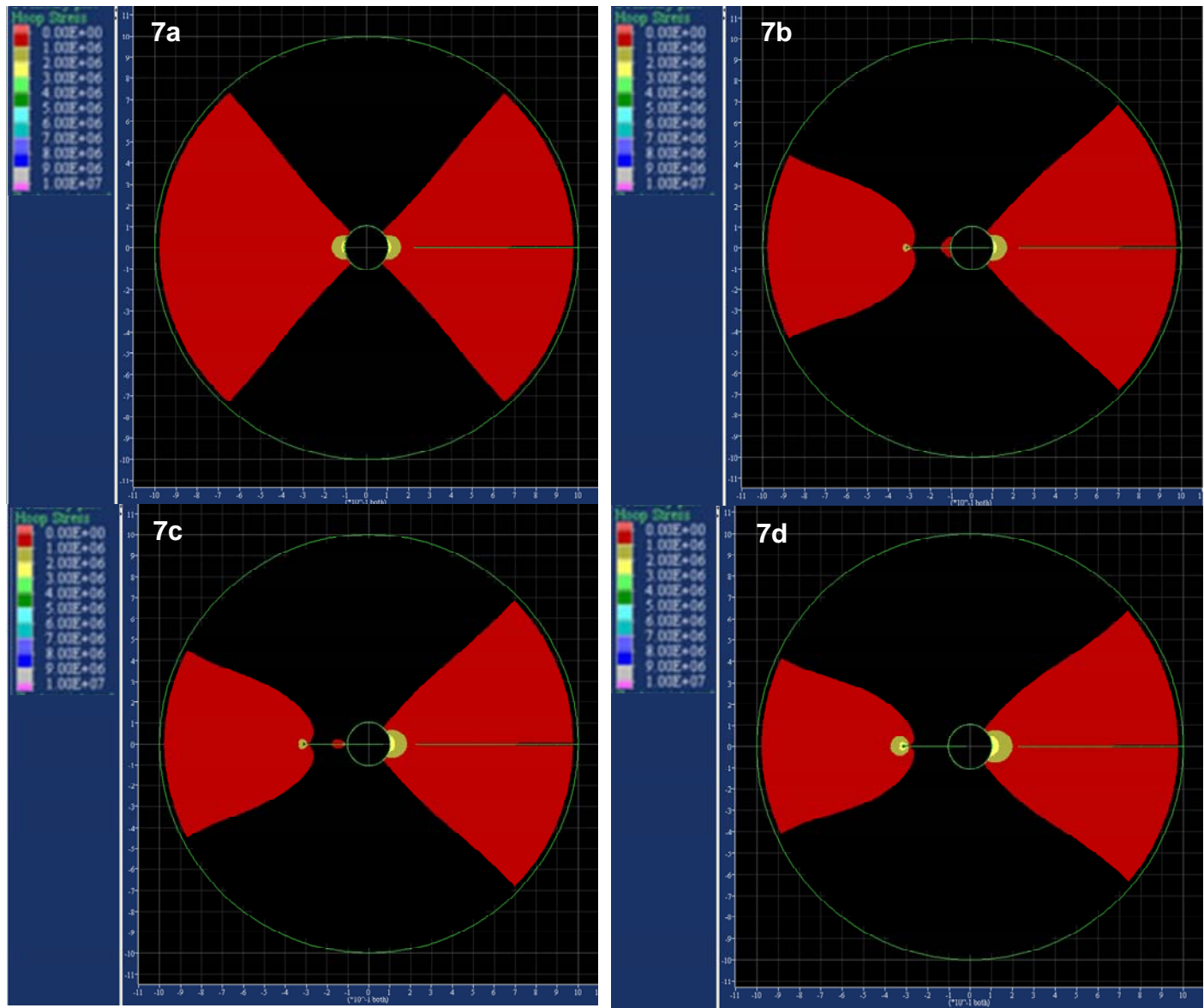


Fig. 7 – Tensile hoop stress distribution around the borehole and fracture. FLAC-2D simulations assuming shale properties in Table 1. Black denotes no tensile hoop stress. Red-yellow-green-blue colors denote higher stress. Stress values in key are in Pa ($1 \text{ MPa} = 10^6 \text{ Pa}$); each color change denotes a change in stress by 1 MPa. Positive values denote tensile stress. Minimum horizontal stress, sh_{\min} , oriented N-S; maximum horizontal stress, SH_{\max} , oriented E-W. **Fig. 7a** – Circular borehole; **Fig. 7b** – Circular borehole with unsupported fracture; **Fig. 7c** – Circular borehole with a propped fracture, prop length 9.5 mm; **Fig. 7d** – Circular borehole with a propped fracture, prop length 93 mm.

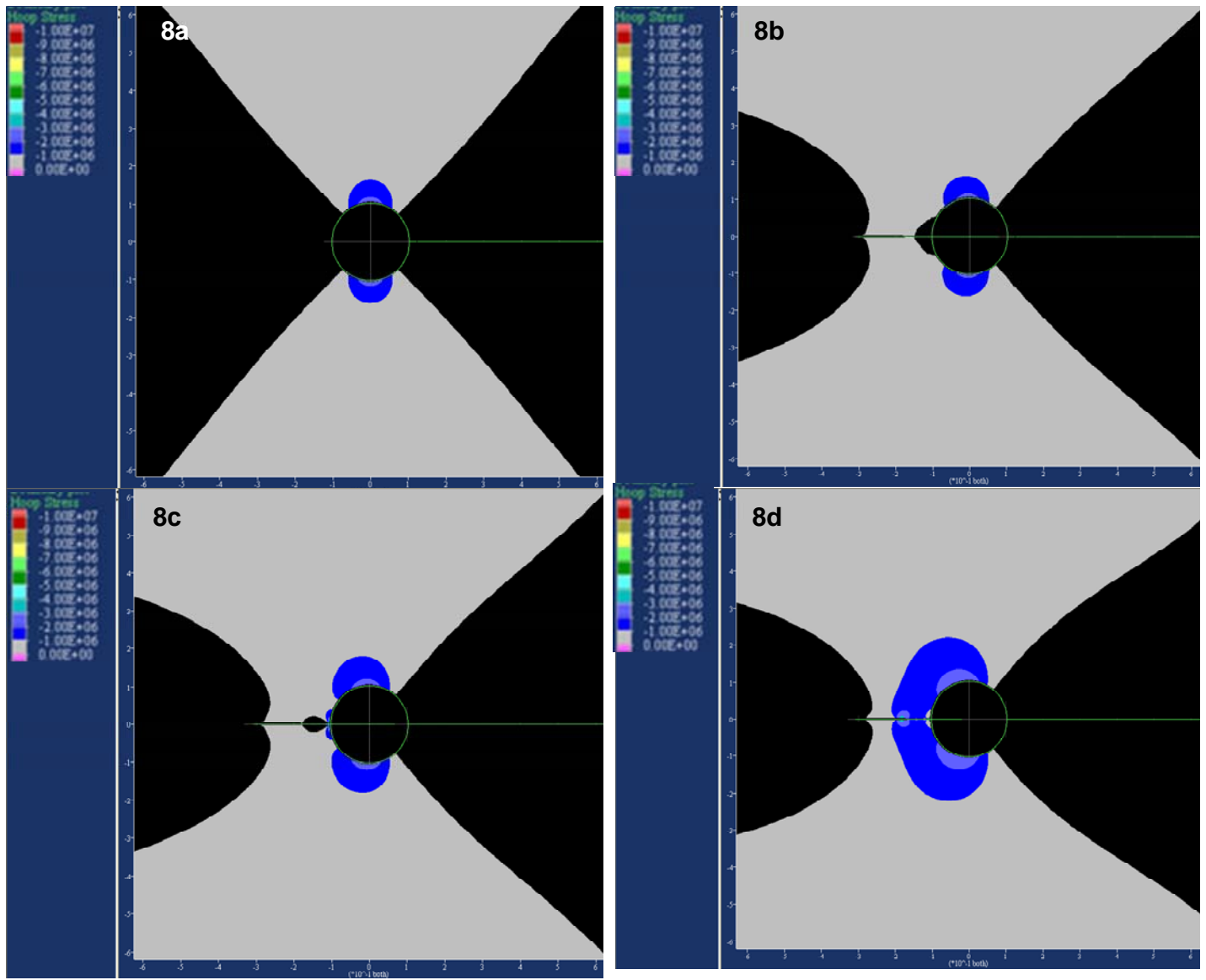


Fig. 8 – Compressive hoop stress distribution around the borehole and fracture. FLAC-2D simulations assuming shale properties in Table 1. Black denotes no compressive hoop stress. Yellow-blue-pink colors denote higher stress. Stress values in key are in Pa ($1 \text{ MPa} = 10^6 \text{ Pa}$); each color change denotes a change in stress by 1 MPa. Negative values denote compressive stress. Minimum horizontal stress, sh_{\min} , oriented N-S; maximum horizontal stress, SH_{\max} , oriented E-W. **Fig. 8a** – Circular borehole; **Fig. 8b** – Circular borehole with unsupported fracture; **Fig. 8c** – Circular borehole with a propped fracture, prop length 9.5 mm; **Fig. 8d** – Circular borehole with a propped fracture, prop length 93 mm.

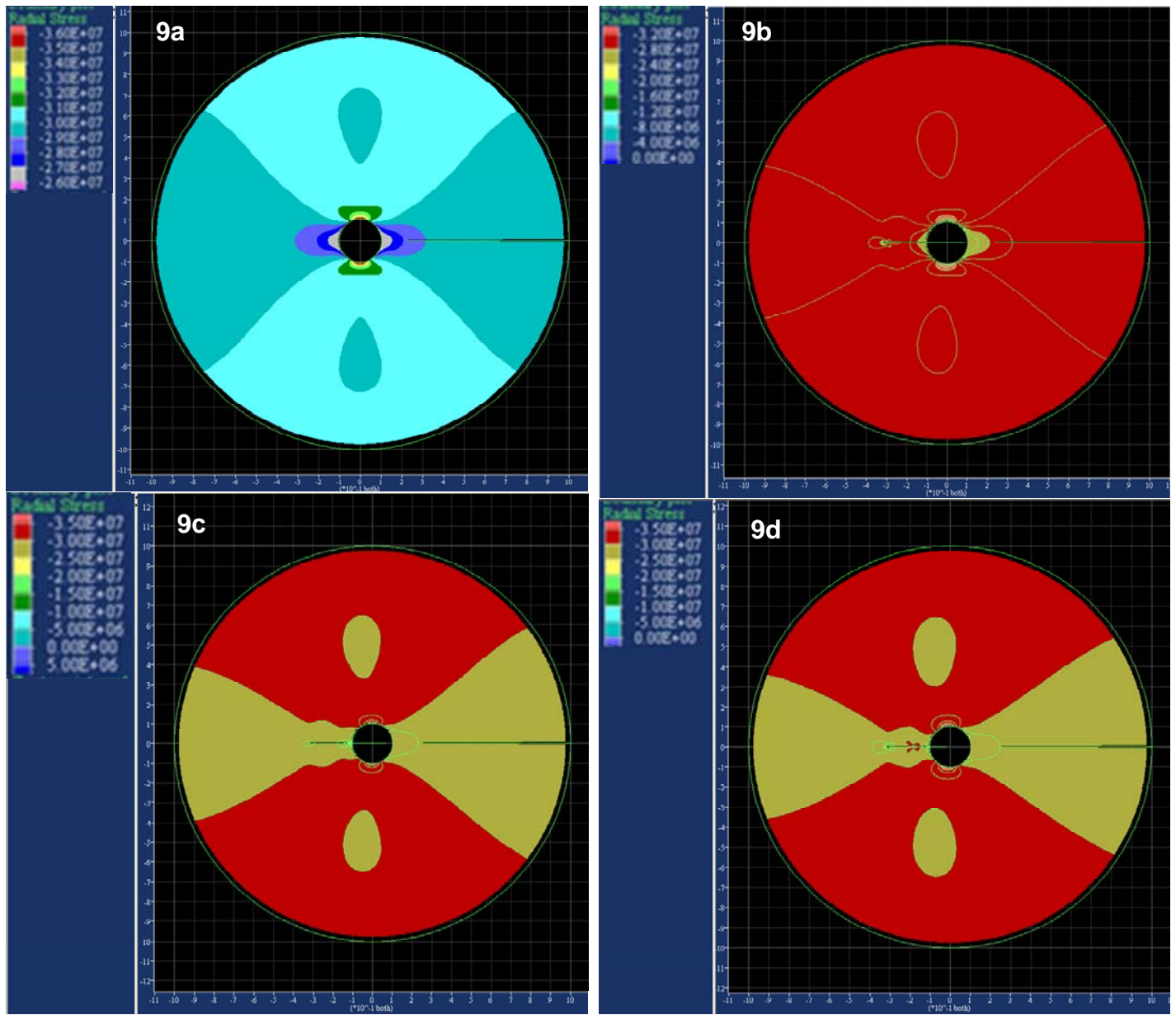


Fig. 9 – Radial stress distribution around the borehole and fracture. FLAC-2D simulations assuming shale properties in Table 1. Yellow-beige-red shades denote increasing radial stress; scales vary in each figure. Stress values in key are in Pa (1 MPa = 10^6 Pa). Positive values denote tensile stress and negative values denote compressive stress. Minimum horizontal stress, sh_{min} , oriented N-S; maximum horizontal stress, SH_{max} , oriented E-W. **Fig. 9a** – Circular borehole; **Fig. 9b** – Circular borehole with unsupported fracture; **Fig. 9c** – Circular borehole with a propped fracture, prop length 9.5 mm; **Fig. 9d** – Circular borehole with a propped fracture, prop length 93 mm.

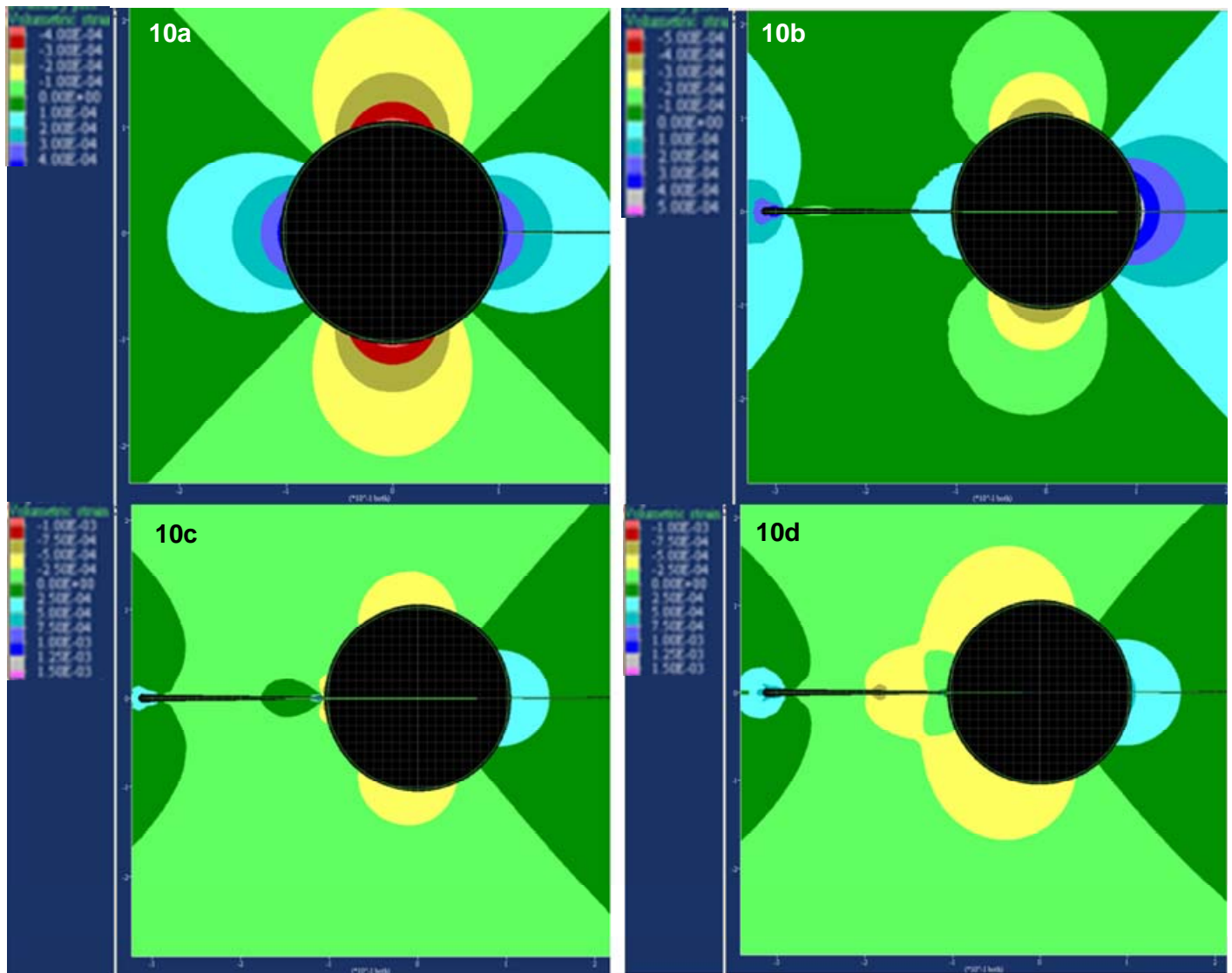


Fig. 10 – Volumetric strain around the borehole and fracture. FLAC-2D simulations assuming shale properties presented in Table 1. Yellow-red shades (negative values) denote volumetric compression; green-blue shades (positive values) indicate volumetric expansion (dilation). Scales vary in each figure. Strain values in key are in Percent (1 microStrain = 10^{-3} Strain%). Minimum horizontal stress, sh_{min} , oriented N-S; maximum horizontal stress, SH_{max} , oriented E-W. **Fig. 10a** – Circular borehole; **Fig. 10b** – Circular borehole with unsupported fracture; **Fig. 10c** – Circular borehole with a propped fracture, prop length 9.5 mm; **Fig. 10d** – Circular borehole with a propped fracture, prop length 93 mm.

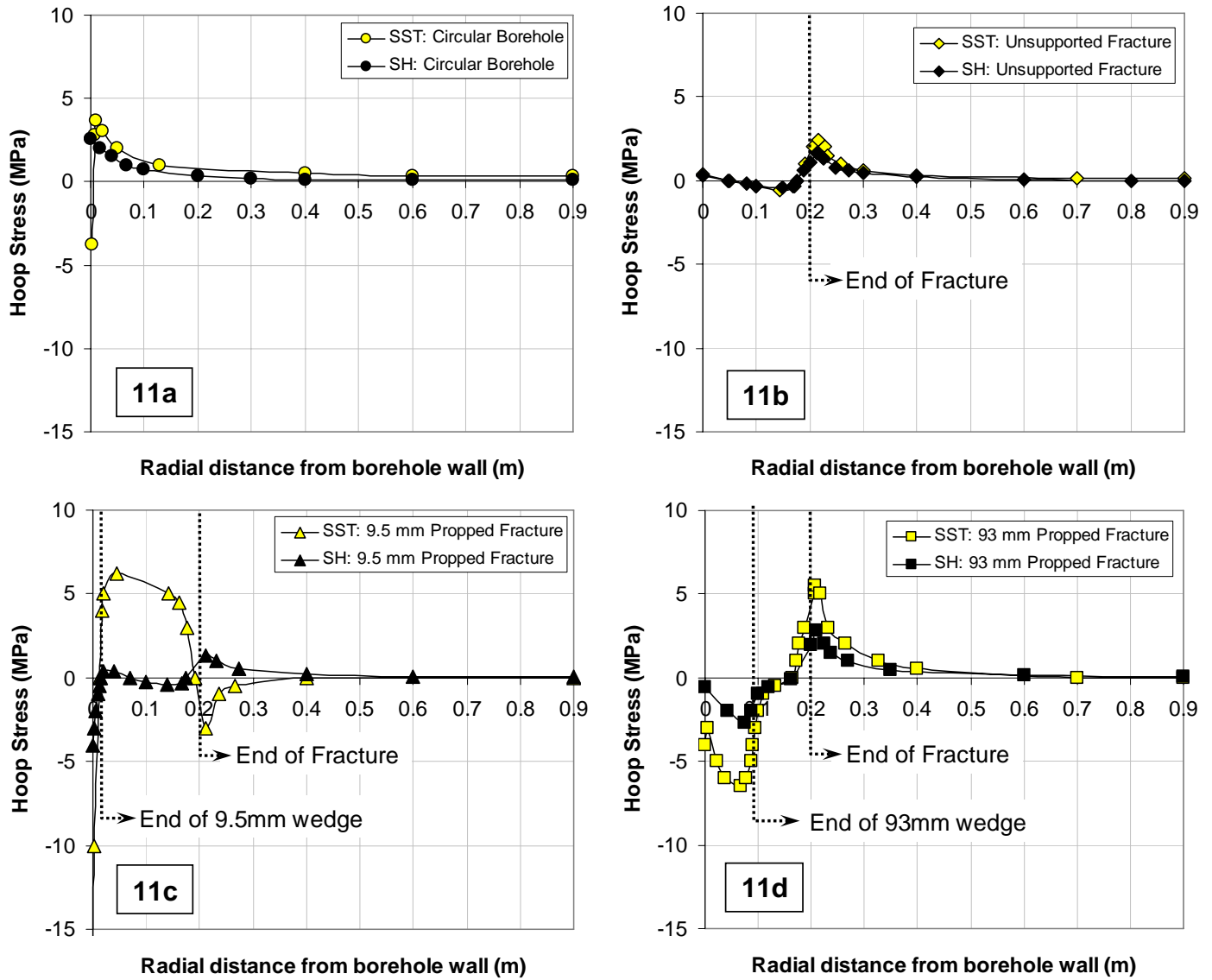


Fig. 11 – Profile of the hoop stress with respect to radial distance from the wellbore wall. The data have been extracted from the FLAC-2D simulations assuming sandstone and shale properties in Table 1 and compare directly with Figures 3, 4, 7 and 8. Negative values denote compressive stress; positive values denote tensile stress. **Fig. 11a** – Circular borehole; **Fig. 11b** – Circular borehole with unsupported fracture; **Fig. 11c** – Circular borehole with a propped fracture, prop length 9.5 mm; **Fig. 11d** – Circular borehole with a propped fracture, prop length 93 mm.